

SCIENTIFIC REPORTS



OPEN

Synchronization in slowly switching networks of coupled oscillators

Jie Zhou¹, Yong Zou¹, Shuguang Guan¹, Zonghua Liu¹ & S. Boccaletti^{2,3}

Received: 13 July 2016

Accepted: 07 October 2016

Published: 25 October 2016

Networks whose structure of connections evolves in time constitute a big challenge in the study of synchronization, in particular when the time scales for the evolution of the graph topology are comparable with (or even longer than) those pertinent to the units' dynamics. We here focus on networks with a slow-switching structure, and show that the necessary conditions for synchronization, i.e. the conditions for which synchronization is locally stable, are determined by the time average of the largest Lyapunov exponents of transverse modes of the switching topologies. Comparison between fast- and slow-switching networks allows elucidating that slow-switching processes prompt synchronization in the cases where the Master Stability Function is concave, whereas fast-switching schemes facilitate synchronization for convex curves. Moreover, the condition of slow-switching enables the introduction of a control strategy for inducing synchronization in networks with arbitrary structure and coupling strength, which is of evident relevance for broad applications in real world systems.

Synchronization plays a crucial role in a wide spectrum of technological, biological, and social networks^{1–4}. Even though studied intensively under various aspects^{5–11}, yet a full clarification is needed on the effects of time-dependent coupling structures^{12–16}, particularly for those circumstances for which the coupling strengths (or connection topologies) may switch in time. For the specific condition (termed as the *blinking network* case) for which the graph structure changes much more rapidly than the units' dynamics, a comprehensive theoretical framework was established, and applications were developed accordingly^{17–19}. However, such an extreme situation does not properly match the generic case, as in the majority of real-world systems the time scale for the coupling evolution turns out to be in fact secular with respect to that of the individual dynamics. For instance, the time scales of synaptic plasticity (the basis of most models in neural circuits) is known to expand from milliseconds to days^{20–23}, and long term plasticity between neurons is actually thought to be the real clue for the higher level functioning of the brain, such as long term memory²⁴. A further example is evolutionary processes leading to mutations in genetic networks, which evidently take place over timescales much longer than those related to genetic expressions. Moreover, based on minimal models of interacting binary state nodes, different time scales of coupling switching may even lead the network into distinct phases of collective behavior²⁵.

Synchronization in slow-switching networks calls still for a general theory, and for elucidation. Despite the importance of the issue, current studies are so far limited to either simple unit dynamics (e.g. linear system²⁶), or simple coupling dynamics (e.g. on-off coupling^{27,28}), or continuous switching processes²⁹. In this paper, we provide instead the general criteria for stable synchronization in slowly varying networked systems, and demonstrate that the stability of synchronization is fully characterized by the largest Lyapunov exponents of the transverse modes associated to the varying structures. Comparison to the fast-switching case allows to show that enhancement of synchronization can be predicted from the profile of the master stability function (MSF). Moreover, a network controlling strategy can be sorted out from our results, which embeds a controlling structure into the system, predesigned as a standard one (i.e. regardless of the specific topology to be controlled), in a way that it may find applications even to systems whose structures are unknown.

Model and Theory

We start by considering a networked system with N identical systems, described as $\dot{\mathbf{x}}^i = \mathbf{F}(\mathbf{x}^i)$, with $i = 1, 2, \dots, N$, $\mathbf{x}^i \in \mathbb{R}^m$, and $\mathbf{F}: \mathbb{R}^m \rightarrow \mathbb{R}^m$. The units interact with their neighbors, so that the dynamics of the i -th node is ruled by $\dot{\mathbf{x}}^i = \mathbf{F}(\mathbf{x}^i) - \sigma \sum_j g_{ij} \mathbf{H}(\mathbf{x}^j)$, where σ is the coupling strength, g_{ij} is the element of Laplacian \mathbf{G} , and

¹Department of Physics, East China Normal University, Shanghai 200241, China. ²CNR-Institute of Complex Systems, Via Madonna del Piano, 10, 50019 Sesto Fiorentino, Florence, Italy. ³The Embassy of Italy in Tel Aviv, 25 Hamered street, 68125 Tel Aviv, Israel. Correspondence and requests for materials should be addressed to J.Z. (email: jzhou@phy.ecnu.edu.cn) or S.B. (email: stefano.boccaletti@gmail.com)

$\mathbf{H}: \mathbb{R}^m \rightarrow \mathbb{R}^m$ specifies the output function through which coupling is realized among the networks' units. Let furthermore $\mathbf{x}^1 = \mathbf{x}^2 = \dots = \mathbf{x}^N \equiv \mathbf{x}^S$ be the synchronized solution and $\delta \mathbf{x}^i \equiv \mathbf{x}^i - \mathbf{x}^S$ the m dimensional vector accounting for the deviation in time between the evolution of the network's node i and the synchronized state.

For static networks (i.e. when \mathbf{G} does not change in time), the linearized equation of the system (around \mathbf{x}^S) is expressed as

$$\delta \dot{\mathbf{x}} = [\mathbf{I}_N \otimes D\mathbf{F} - \sigma \mathbf{G} \otimes D\mathbf{H}] \delta \mathbf{x}, \tag{1}$$

where $\delta \mathbf{x} = (\delta x^1, \dots, \delta x^N)^T$, and $D\mathbf{F}$ and $D\mathbf{H}$ are the Jacobian functions of \mathbf{F} and \mathbf{H} , respectively, evaluated on the synchronized solution \mathbf{x}^S . By plugging $\mathbf{G} = \sum_{j=1}^N \lambda^j \mathbf{u}^j \mathbf{u}^{jT}$ into Eq. (1) (where $\lambda^1 = 0 < \lambda^2 < \dots < \lambda^N$ are the eigenvalues and $\{\mathbf{u}^j\}$ the corresponding eigenvectors providing an orthonormal basis of \mathbb{R}^N), and setting $\delta \mathbf{x}(t) = \mathbf{Q} \delta \mathbf{y}(t)$ [with $\mathbf{Q} = (\mathbf{u}^1, \dots, \mathbf{u}^N) \otimes \mathbf{I}_m$] and $\delta \mathbf{y} = (\delta y^1, \dots, \delta y^N)^T$, one obtains

$$\delta \dot{\mathbf{y}}^j = (D\mathbf{F} - \sigma \lambda^j D\mathbf{H}) \delta \mathbf{y}^j. \tag{2}$$

The largest Lyapunov exponent of the transverse mode $\delta \mathbf{y}^j$ is defined as

$$\Phi(\sigma \lambda^j) = \lim_{t \rightarrow \infty} \frac{1}{t} \ln \frac{|\delta \mathbf{y}^j(t)|}{|\delta \mathbf{y}^j(0)|}, \tag{3}$$

which is a function of the eigenvalue λ^j and coupling strength σ , also known as the Master Stability Function (MSF). The necessary condition for having a stable synchronization is that MSF $\Phi(\sigma \lambda^j)$ is negative for all the transverse modes $j \geq 2$, as elaborated in ref. 11.

Now, let us consider the case of time-varying networks where the Laplacian \mathbf{G} is composed of a sequence of coupling matrices $(\mathbf{G}_1, \mathbf{G}_2, \dots)$ that occur in a chronological order. Suppose, further, that \mathbf{G}_k lasts for a lapse τ_k under coupling strength σ_k (a condition that we will denote as $\{\mathbf{G}_k, \tau_k, \sigma_k\}$). Then $\mathbf{G}(t)$ is represented by $\mathbf{G}(t) = (\{\mathbf{G}_1, \tau_1, \sigma_1\}, \{\mathbf{G}_2, \tau_2, \sigma_2\}, \dots)$.

To elucidate the effect of a slow switching, we start from the simplest case that the network alternates between two structures $(\mathbf{G}_1$ and $\mathbf{G}_2)$, so that the system periodically switches between configurations $\{\mathbf{G}_1, \tau_1, \sigma_1\}$ and $\{\mathbf{G}_2, \tau_2, \sigma_2\}$, with a period $T = \tau_1 + \tau_2$. Again taking $\mathbf{G}_1 = \sum_{j=1}^N \lambda_1^j \mathbf{u}^j \mathbf{u}^{jT}$ and $\mathbf{G}_2 = \sum_{l=1}^N \lambda_2^l \mathbf{v}^l \mathbf{v}^{lT}$, one obtains that the necessary condition of stable synchronization is the following: for each pair of transverse modes $(j, l \geq 2)$, if $S_{jl} \neq 0$ where $S_{jl} = \mathbf{v}^{lT} \mathbf{u}^j$, one should have (see Methods, part I for details)

$$\tau_1 \Phi(\sigma_1 \lambda_1^j) + \tau_2 \Phi(\sigma_2 \lambda_2^l) < 0. \tag{4}$$

The condition is readily extended to the general case of a network that slowly switches among a sequence of L configurations, i.e. $(\{\mathbf{G}_1, \tau_1, \sigma_1\}, \dots, \{\mathbf{G}_L, \tau_L, \sigma_L\})$ with $\mathbf{G}_k = \sum_{j=1}^N \lambda_k^j \mathbf{u}_k^j \mathbf{u}_k^{jT}$: for each combination of the transverse modes of the L configurations (j_1, j_2, \dots, j_L) , if all the $L - 1$ pairs of vectors $(\mathbf{u}_k^{j_k}, \mathbf{u}_{k-1}^{j_{k-1}})$ ($2 \leq k \leq L$) are non-orthogonal, one should have

$$\sum_{k=1}^L \tau_k \Phi(\sigma_k \lambda_k^{j_k}) < 0. \tag{5}$$

With the conditions (4, 5), for any function $\mathbf{F}: \mathbb{R}^m \rightarrow \mathbb{R}^m$ the MSF $\Phi(\sigma \lambda^j)$ is, indeed, obtained straightforwardly, and once one has the specific sets of eigenvalues and eigenvectors that diagonalize the L configurations, the specific values of $\Phi(\sigma_k \lambda_k^{j_k})$ can be simply read on the *unique* MSF for each $2 \leq k \leq L$, so that predictions on the stability of synchronization can be elegantly made by checking whether conditions (4, 5) are fulfilled. In the following, we will therefore linger on some practical applications of our theory.

Results

In this paper, we consider the case of Rössler oscillators where the unit dynamics is described by $\dot{x}_1^i = -(x_2^i + x_3^i)$, $\dot{x}_2^i = x_1^i + a x_3^i$, $\dot{x}_3^i = b + x_3^i(x_1^i - c)$ with $\mathbf{x}^i = (x_1^i, x_2^i, x_3^i)^T$ and parameters being $a = b = 0.2$, and $c = 7$. \mathbf{H} is a 3×3 matrix, whose elements are 1 for h_{11} and 0 otherwise, i.e it realizes a linear coupling on the x_1 variable of the graph's units. Dynamics is integrated with a fixed time step $\Delta t = 0.001$, and the synchronization performance is evaluated by the error function defined as

$$\langle \delta \rangle = \left\langle \frac{\sum_{i=2}^N (|x_1^i - x_1^1| + |x_2^i - x_2^1| + |x_3^i - x_3^1|)}{3(N - 1)} \right\rangle, \tag{6}$$

where $\langle \cdot \rangle$ denotes the time average over a sufficient long time after discarding transient processes.

Validation of Analytic Predictions. To validate the analytic prediction, we first consider a simple case of a network made of just three oscillators, which switches between two structures along the same time interval τ . The Laplacians of the two connection arrangements are $\mathbf{G}_1 = \sum_{j=1}^3 \lambda_1^j \mathbf{u}^j \mathbf{u}^{jT}$ and $\mathbf{G}_2 = \sum_{l=1}^3 \lambda_2^l \mathbf{v}^l \mathbf{v}^{lT}$ with $\mathbf{u}^1 = \mathbf{v}^1 = (1, 1, 1)^T$ and $\lambda_1^1 = \lambda_2^1 = 0$ (which is along the synchronization manifold $\mathbf{x}^1 = \mathbf{x}^2 = \mathbf{x}^3$). For simplicity, we set $\sigma_1 = \sigma_2 = 1$, $\mathbf{u}^2 = \mathbf{v}^2$, and $\mathbf{u}^3 = \mathbf{v}^3$, and thus $S_{jl} = \delta_{jl}$. According to Eq. (4), the system is stable on the synchronization manifold when $\Phi(\lambda_1^j) + \Phi(\lambda_2^j) < 0$ for $j = 2$ and 3 , respectively. Figure 1(a) reports the synchronization index $\langle \delta \rangle$ in the $(\lambda_2^2, \lambda_2^3)$ plane, where the values of λ_1^2 and λ_1^3 are fixed as 3. Notice that the solid lines [obtained

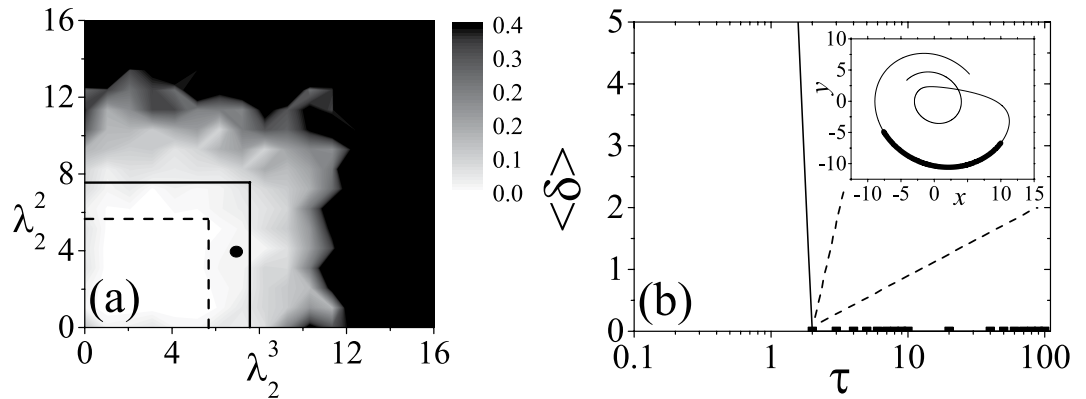


Figure 1. (a) Gray plot of $\langle \delta \rangle$ in the $(\lambda_2^2, \lambda_2^3)$ plane, for $\lambda_1^2 = \lambda_1^3 = 3$ and $\sigma_1 = \sigma_2 = 1$. Solid lines indicate the predicted boundaries of the synchronization region. Dashed lines indicate the boundaries for the case of fast switching. $\mathbf{u}^2 = \mathbf{v}^2 = (1, -2, 1)^T / \sqrt{6}$, and $\mathbf{u}^3 = \mathbf{v}^3 = (1, 0, -1)^T / \sqrt{2}$. (b) $\langle \delta \rangle$ vs. τ for the case $\lambda_2^2 = 4$ and $\lambda_2^3 = 7$ [indicated by a solid dot in panel (a)]. Inset: Thick black curve shows a typical trajectory of the Rössler oscillator projected on xy -plane for the lapse of time $\tau = 2$. Thin line reports the actual continuation of that trajectory, and serves as a guide for eye.

from the equations $\Phi(\lambda_1^j) + \Phi(\lambda_2^j) = 0$ for $j = 2$ and 3 , respectively] separate the plane into two regions: the white one (synchronized dynamics) and the dark one (asynchronous behavior), in good agreement with the numerical results. It is remarkable that this result is pertinent to a specific choice for the switching time ($\tau = 10$). Since this result pertains to the slow-switching scenario, it is worth exploring the range of τ for which the overall scenario is actually maintained. Figure 1(b) reports $\langle \delta \rangle$ vs. τ , for $\lambda_2^2 = 4$ and $\lambda_2^3 = 7$ [the solid spot in (a)]. $\langle \delta \rangle$ vanishes for $\tau \geq 2$, whereas it diverges for $\tau < 2$ (i.e. when the structures start to switch faster).

In fact, as soon as the switching process occurs over fast enough time scales, a sufficient condition is that the time average of the coupling matrices $\bar{\mathbf{G}} = \frac{1}{T}(\tau_1 \mathbf{G}_1 + \tau_2 \mathbf{G}_2)$ supports synchronization^{17,18}. In particular, when \mathbf{G}_1 and \mathbf{G}_2 share the same basis, i.e. $\mathbf{u}^j = \mathbf{v}^j$ for all j , an equivalent condition for fast-switching networks can be obtained, that is: $\Phi(\frac{\tau_1}{T} \sigma_1 \lambda_1^j + \frac{\tau_2}{T} \sigma_2 \lambda_2^j) < 0$ for $2 \leq j \leq N$ (see Methods, part II for details). For comparison, this latter condition is reported with dashed lines in Fig. 1(a). As the region delimited by the dashed lines is embraced in that contoured by solid lines, we may conclude that in this case a slow switching scheme is prompting synchronization more than a fast switching one.

The Shape of Master Stability Function. A second remarkable application is the prediction, under fixed topology and switching coupling strengths, of the most favorable switching scheme for synchronization. The conditions of slow (large τ) and fast (small τ) switching schemes lead, indeed, to a general criterion for a class of networks whose coupling strength may vary with time while the Laplacian \mathbf{G} is fixed, for example networks with on-off coupling²⁷. Specifically, for the case that the coupling strength switches between two values σ_1 and σ_2 alternatively, the criterion (which can be readily extended to general case of arbitrary number of different values) can be stated as follows: when the MSF is *concave* in the domain spanned by the Laplacian eigenvalues, i.e. $\alpha \Phi(x_1) + (1 - \alpha) \Phi(x_2) \leq \Phi[\alpha x_1 + (1 - \alpha)x_2]$, if the network supports a synchronous dynamics under a fast switching [i.e. $\Phi(\frac{\tau_1}{T} \sigma_1 \lambda^j + \frac{\tau_2}{T} \sigma_2 \lambda^j) < 0$ ($\forall j \geq 2$)], the same network will also behave synchronously under slow switching of the same structures [i.e. $\frac{\tau_1}{T} \Phi(\sigma_1 \lambda^j) + \frac{\tau_2}{T} \Phi(\sigma_2 \lambda^j) < 0$ ($\forall j \geq 2$)]. When instead the MSF is *convex*, the situation is reversed, and slow switching conditions include the fast switching ones.

In order to better elucidate the above relationship between the two switching schemes, we take the case of a complete network, for which all non-vanishing eigenvalues of the Laplacian are the same, $\lambda^2 = \lambda^3 = \dots = \lambda^N = N$, so that the $N - 1$ transverse eigenmodes form an $(N - 1)$ -dimensional linear subspace. Specifically, we preserve the network structure as a complete graph, and switch the coupling strength between σ_1 and σ_2 with the same time interval τ , so that the argument $\sigma \lambda$ of the MSF is (for all transverse modes) switched between $\sigma_1 N$ and $\sigma_2 N$. Noting that the associated conditions for stable synchronization are $\Phi(\frac{\sigma_1 N + \sigma_2 N}{2}) < 0$ (fast switching) and $\frac{\Phi(\sigma_1 N) + \Phi(\sigma_2 N)}{2} < 0$ (slow switching).

Figure 2 reports the results for the cases of $\tau = \Delta t = 0.001$ (fast switching, panel (a)) and $\tau = 10^4 \Delta t = 10$ (slow switching, panel (b)), where σ_1 is fixed at $3/N$ so that $\sigma_1 N = 3$, and $\sigma_2 N$ goes from 3 to 15 (being the MSF concave in the corresponding domain). The MSF for the considered Rössler chaotic dynamics is shown in panels (c) and (d). The long dashed lines crossing panels (a) (red lines) and (b) (green lines) show the boundaries of $\sigma_2 N$ for synchronization, coming from the conditions $\Phi(\frac{3 + \sigma_2 N}{2}) = 0$ and $\frac{\Phi(3) + \Phi(\sigma_2 N)}{2} = 0$, respectively. Dashed lines in (c) and (d) indicate how one can predict the boundaries with just the help of the shape of the MSF (details in the caption). Theory and the numerical results match very well. It is clearly shown that the range spanned by the green dashed lines in panel (d) is larger than that spanned by the red dashed line in panel (c), which confirms the our conclusion that when the MSF is concave in the domain concerned, the case of slow switching allows

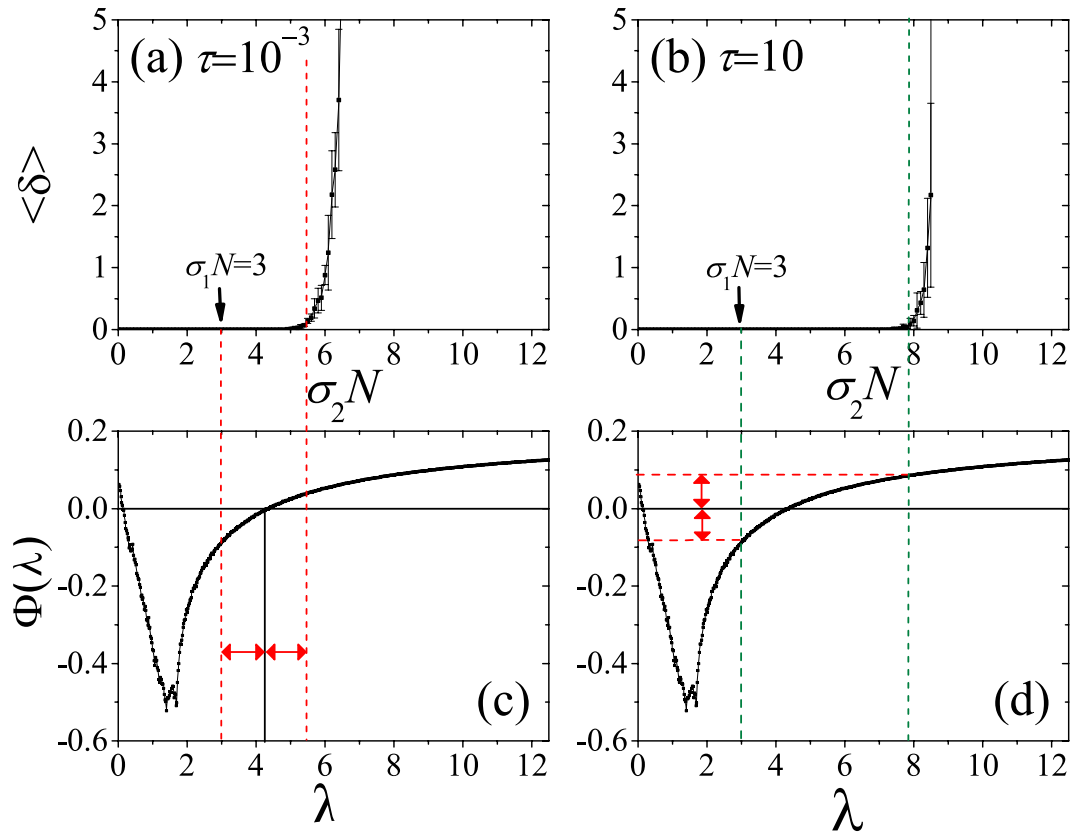


Figure 2. Upper panels: $\langle \delta \rangle$ vs. $\sigma_2 N$ for $\tau = 10^{-3}$ [fast switching, panel (a)] and $\tau = 10$ [slow switching, panel (b)]. $N = 100$ and $\sigma_1 N = 3$. Lower panels: the MSF corresponding to our choice of the Rössler chaotic oscillator. In panel (c), the red dashed lines pointed by the red arrows indicate the value of $\sigma_1 N = 3$ (the left one), and $\sigma_2 N$ which satisfies $\Phi\left(\frac{3 + \sigma_2 N}{2}\right) = 0$ (the right one), therefore giving the equal length of the two arrows. In panel (d), the red dashed lines pointed by the red arrows indicate the value of $\Phi(\sigma_1 N = 3)$ (the lower one), and $\Phi(\sigma_2 N)$ which satisfies $\frac{\Phi(3) + \Phi(\sigma_2 N)}{2} = 0$ (the upper one), and also the equal length of the two arrows. The green dashed lines indicate the corresponding values of $\sigma_1 N = 3$ and $\sigma_2 N$. The results are averaged over 50 realizations.

synchronization for a range of $\sigma_2 N$ larger than that of fast switching. While this example considers explicitly a concave MSF, the case of a convex MSF is described and reported in the Supplementary Information.

A Control Strategy. As a last step of our study, we show how the discovered conditions suggest the realization of controlling strategies for inducing synchronization in generic networks. Specifically, we introduce a heuristic approach, whose main idea is to periodically add a controlling network into a pristine graph, in a way that the whole network switches alternatively between the original topology (i.e. the target network to be controlled) and the controlling structure. This latter structure is actually chosen in order that the resulting time-evolving graph satisfies the conditions for stable synchronization provided in the above. In fact, the spectrum of the Laplacian of the original network may be very different from one to another, with more heterogeneous graphs displaying larger ranges of eigenvalues' spectrum³⁰. Thus, finding a proper controlling structure for each specific original network is a key step in this strategy.

Having to cope with a generic case, we here propose a controlling structure (a graph) for which the non null eigenvalues of the Laplacian are all the same, say λ , and the coupling strength σ is chosen such that $\Phi(\sigma\lambda) = \Phi_{\min}$ (where Φ_{\min} is the minimum value of the MSF). Because the values of MSF for all the transverse modes reach Φ_{\min} , this kind of networks is optimal for synchronization, and we refer to them as *Optimal synchronization networks* (OSN). For binary interaction networks (those represented by adjacency matrices), the number of optional OSNs could be very large. A practical way of constructing an OSN is provided in ref. 31.

Now suppose that, during each period, the pristine network stays fixed for a time τ_U , and then the system switches to an OSN which remains fixed for a time τ_O . Noted that, regardless the specific spectrum of the original graph, the possible values of Φ will never exceed the maximum value of the MSF, Φ_{\max} . Therefore, according to our condition for slow switching, the graph will be controlled when $\tau_O/\tau_U \geq \Phi_{\max}/|\Phi_{\min}|$, no matter what its structure is. For our specific choice of Rössler system, $\Phi_{\max} \simeq 2.0$ and $\Phi_{\min} \simeq -5.0$, one may expect that *any* network can be controlled when $\tau_O/\tau_U \geq \Phi_{\max}/|\Phi_{\min}| \simeq 0.4$.

To validate our predictions, we generate homogeneous and heterogenous networks of size $N = 100$ by means of the Erdős-Rényi (ER³²) and Barabási-Albert (BA³³) models, and adopt complete networks as controlling

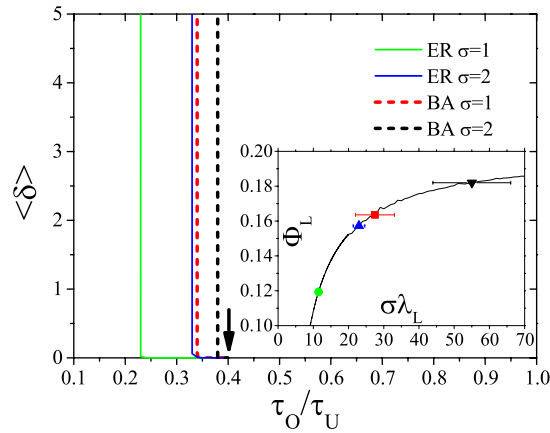


Figure 3. $\langle \delta \rangle$ as a function of the ratio τ_O/τ_U with τ_O fixed at $\tau_O = 10$, for ER and BA networks with different coupling strength σ (see the legend for the color code). The arrow indicates the value of $\Phi_{\max}/|\Phi_{\min}| \simeq 0.4$. The inset shows the largest MSF value Φ_L of these networks. The reported results refer to ensemble averages over 50 different realizations.

structures (other choices of OSNs were considered and similar results, not shown here, were obtained). According to the condition for slow switching, the threshold of the ratio τ_O/τ_U for the controlling procedure is fully determined by the transverse mode which has the largest MSF value among all the others. By denoting the largest MSF value reached by this mode as Φ_L , the synchronization condition requires $\tau_O/\tau_U \geq \Phi_L/|\Phi_{\min}|$. The inset of Fig. 3 reports the values of Φ_L . When $\sigma = 1$, Φ_L is relatively small for both ER and BA networks, and therefore the graphs can be controlled with a small ratio $\tau_O/\tau_U (\geq \Phi_L/|\Phi_{\min}|)$, as shown in the main panel of Fig. 3. When $\sigma = 2$, the value of Φ_L increases, and a larger ratio of τ_O/τ_U is needed. However, a further increase in σ leads to the saturation of Φ_L at Φ_{\max} , and to the convergence of the ratio τ_O/τ_U to the expected threshold value (about 0.4), as indicated by the arrow in the main panel of the figure.

Discussion

In conclusion, we succeeded in setting the necessary condition for stable synchronization of slowly switching networks. Together with the criterion of fast switching networks in previous works, the both ends of the related condition of switching networks now have been filled. As a contrast to fast switching networks, for slowly switching networks, the condition of stable synchronization is affected by the largest Lyapunov exponent of each transversal mode of switching structures rather than that of their aggregation. Interestingly, we find that such difference in the two switching schemes help us, with the shape of the Master stability function (MSF), in predicting which switching scheme is more favourable for synchronization. Specifically, when the MSF is concave (convex) in the domain the argument span, the network supports a synchronous dynamic under a fast (slow) switching, the same network also behaves synchronously under slow (fast) switching of the same structures. This result further exploits the information embedded in the MSF, from the number and positions of the null points to the shape of it.

The results about slow switching networks may provide potential applications. In this paper, we propose a heuristic controlling strategy according to the characteristic of slow switching networks, where a controlling structure is inserted to the target network periodically. To make this strategy to be general for different situations, we introduce the optimal synchronization networks (OSN) (graphs whose largest Lyapunov exponents of all the transversal modes are close to the minimum value of the Master Stability Function) and show that they serve as an excellent class of controlling networks. In particular, with the knowledge of MSF, the ratio between the action times of OSN and target networks could be preassigned as a standard, and the target networks could be controlled regardless of their specific structure or coupling strength. Therefore, this strategy has potential applications to a wide variety of systems, with unbounded coupling and unknown structure.

We highlight that the obtained condition of stable synchronization is *necessary* but not *sufficient*, which roots from the fundamental limitation of MSF which only assesses local stability of the synchronized state. Sufficient conditions may, in limited situations, be derived from global stability analysis, such as Lyapunov function methods.

Methods

Condition of stable synchronization of slowly switching networks. Let us start from the original case of a network which is fixed on a single structure. While the condition, for this case, has been obtained by Pecora *et al.* in ref. 11, we shall further elaborate on the details of the analytic procedure, which will be helpful to further understand the general case of slow-switching networks.

The linearized equation of the system deviating around the solution $\mathbf{x}^s \equiv \mathbf{x}^1 = \mathbf{x}^2 = \dots = \mathbf{x}^N$ is expressed as

$$\delta \dot{\mathbf{x}} = [\mathbf{I}_N \otimes D\mathbf{F} - \sigma \mathbf{G} \otimes D\mathbf{H}] \delta \mathbf{x}, \quad (7)$$

where the meaning of the notations are the same as those in the main text. The Laplacian \mathbf{G} could be decomposed as $\mathbf{G} = \sum_{j=1}^N \lambda^j \mathbf{u}^j \mathbf{u}^{jT}$ where $\{\lambda^j\}$ is the spectrum with $\lambda_1 = 0$ and $\{\mathbf{u}^j\}$ the eigenvectors with \mathbf{u}^1 corresponding to the synchronization manifold. Taking now \mathbf{I}_N as $\mathbf{I}_N = \sum_{j=1}^N \mathbf{u}^j \mathbf{u}^{jT}$, one gets

$$\delta \mathbf{x} = \sum_{j=1}^N [\mathbf{u}^j \mathbf{u}^{jT} \otimes (D\mathbf{F} + \sigma \lambda^j D\mathbf{H})] \delta \mathbf{x}. \tag{8}$$

Setting $\delta \mathbf{x}(t) = \mathbf{Q} \delta \mathbf{y}(t)$ with $\mathbf{Q} = (\mathbf{u}^1, \dots, \mathbf{u}^N) \otimes \mathbf{I}_m$, Eq. (8) becomes

$$\begin{aligned} \delta \mathbf{y} &= \mathbf{Q}^{-1} \sum_{j=1}^N [\mathbf{u}^j \mathbf{u}^{jT} \otimes (D\mathbf{F} + \sigma \lambda^j D\mathbf{H})] \mathbf{Q} \delta \mathbf{y} \\ &= \sum_{j=1}^N [\mathbf{e}^j \mathbf{e}^{jT} \otimes (D\mathbf{F} + \sigma \lambda^j D\mathbf{H})] \delta \mathbf{y}, \end{aligned} \tag{9}$$

where \mathbf{e}^j is a unit vector whose j -th element is 1 and 0 otherwise. The matrix in Eq. (9) is block diagonal with $m \times m$ blocks. Taking $\delta \mathbf{y}$ as $\delta \mathbf{y} = (\delta \mathbf{y}^1, \dots, \delta \mathbf{y}^N)$ with $\delta \mathbf{y}^j \in \mathbb{R}^m$, one has

$$\delta \mathbf{y}^j = (D\mathbf{F} + \sigma \lambda^j D\mathbf{H}) \delta \mathbf{y}^j. \tag{10}$$

Generally, $D\mathbf{F} + \sigma \lambda^j D\mathbf{H}$ varies with the evolution of the state \mathbf{y}^j , so we can denote $D\mathbf{F} + \sigma \lambda^j D\mathbf{H}$ as $\mathbf{J}_{\sigma \lambda^j}(\mathbf{y}^j)$. Since $\lim_{\Delta t \rightarrow 0} \delta \mathbf{y}^j(t + \Delta t) = \delta \mathbf{y}^j(t) + \Delta t \cdot \dot{\delta \mathbf{y}^j}(t)$, the solution of $\delta \mathbf{y}^j$ can be expressed as

$$\begin{aligned} \delta \mathbf{y}^j(t) &= \lim_{M \rightarrow \infty} \prod_{l=0}^{M-1} [\mathbf{I} + \Delta t \cdot \mathbf{J}_{\sigma \lambda^j}(\mathbf{y}_l^j)] \cdot \delta \mathbf{y}^j(0) \\ &= \lim_{M \rightarrow \infty} \prod_{l=0}^{M-1} \exp[\Delta t \cdot \mathbf{J}_{\sigma \lambda^j}(\mathbf{y}_l^j)] \cdot \delta \mathbf{y}^j(0) \\ &= \lim_{M \rightarrow \infty} \{\exp[\Delta t \cdot \mathbf{J}_{\sigma \lambda^j}(\mathbf{y}_{M-1}^j)] \cdots \exp[\Delta t \cdot \mathbf{J}_{\sigma \lambda^j}(\mathbf{y}_0^j)]\} \cdot \delta \mathbf{y}^j(0), \end{aligned} \tag{11}$$

where $\delta \mathbf{y}^j(0)$ is the initial condition, $\Delta t = t/M$, and $\mathbf{y}_l^j = \mathbf{y}^j(l \cdot \Delta t)$. The $M \rightarrow \infty$ limit procedure gives the formal integral

$$\delta \mathbf{y}^j(t) = \exp\left[\mathbb{L} \int_0^t d\tau \mathbf{J}_{\sigma \lambda^j}(\mathbf{y}^j(\tau))\right] \delta \mathbf{y}^j(0), \tag{12}$$

where \mathbb{L} stands for time-ordered integration, reflecting the continuum limit of the successive left multiplications in Eq. (11). Denoting $\bar{\mathbf{J}}(\sigma \lambda^j) = \frac{1}{t} \mathbb{L} \int_0^t d\tau \mathbf{J}_{\sigma \lambda^j}(\mathbf{y}^j(\tau))$, Eq. (12) becomes

$$\delta \mathbf{y}^j(t) = \exp[\bar{\mathbf{J}}(\sigma \lambda^j) \cdot t] \delta \mathbf{y}^j(0). \tag{13}$$

Now, for ergodic systems, $\bar{\mathbf{J}}(\sigma \lambda^j)$ is asymptotically (i.e. at large enough t) independent of t , and

$$|\delta \mathbf{y}^j(t)| = \|\exp[\bar{\mathbf{J}}(\sigma \lambda^j) \cdot t]\| \cdot |\delta \mathbf{y}^j(0)|. \tag{14}$$

Therefore, if one defines as the largest Lyapunov exponent associated to the j -th eigen-mode

$$\Phi(\sigma \lambda^j) = \lim_{t \rightarrow \infty} \frac{1}{t} \ln \frac{|\delta \mathbf{y}^j(t)|}{|\delta \mathbf{y}^j(0)|}, \tag{15}$$

one has $\|\exp[\bar{\mathbf{J}}(\sigma \lambda^j) \cdot t]\| = \exp[\Phi(\sigma \lambda^j) \cdot t]$ when t is large. Stable synchronization requires (as a necessary condition) the largest Lyapunov exponents $\Phi(\sigma \lambda^j)$ to be negative for all the transverse eigen-modes ($j \geq 2$).

Finally, according to Eq. (13), the solution of $\delta \mathbf{y}$ is

$$\delta \mathbf{y}(t) = \sum_j \{\mathbf{e}^j \mathbf{e}^{jT} \otimes \exp[\bar{\mathbf{J}}(\sigma \lambda^j) \cdot t]\} \delta \mathbf{y}(0), \tag{16}$$

and therefore

$$\delta \mathbf{x}(t) = \sum_j \{\mathbf{u}^j \mathbf{u}^{jT} \otimes \exp[\bar{\mathbf{J}}(\sigma \lambda^j) \cdot t]\} \delta \mathbf{x}(0). \tag{17}$$

Suppose now that a network periodically switches between two configurations $\{\mathbf{G}_1, \tau_1, \sigma_1\}$ and $\{\mathbf{G}_2, \tau_2, \sigma_2\}$, with τ_1 and τ_2 being the lasting times of the two configurations and σ_1 and σ_2 the coupling strengths, respectively. Similarly to the above, one can decompose \mathbf{G}_1 and \mathbf{G}_2 as $\mathbf{G}_1 = \sum_j \lambda_1^j \mathbf{u}^j \mathbf{u}^{jT}$ and $\mathbf{G}_2 = \sum_j \lambda_2^j \mathbf{v}^j \mathbf{v}^{jT}$. For each period $T = \tau_1 + \tau_2$ (supposing \mathbf{G}_1 acts first), the state $\delta \mathbf{x}$ attained by at time T can be written as

$$\begin{aligned}
 \delta \mathbf{x}(T) &= \sum_l \{ \mathbf{v}^l \mathbf{v}^{lT} \otimes \exp[\bar{\mathbf{J}}(\sigma_2 \lambda_2^l) \cdot t] \} \delta \mathbf{x}(\tau_1) \\
 &= \sum_l \{ \mathbf{v}^l \mathbf{v}^{lT} \otimes \exp[\bar{\mathbf{J}}(\sigma_2 \lambda_2^l) \cdot t] \} \sum_j \{ \mathbf{u}^j \mathbf{u}^{jT} \otimes \exp[\bar{\mathbf{J}}(\sigma_1 \lambda_1^j) \cdot t] \} \delta \mathbf{x}(0) \\
 &= \sum_{j,l} \{ \mathbf{v}^l \mathbf{v}^{lT} \mathbf{u}^j \mathbf{u}^{jT} \otimes \exp[\bar{\mathbf{J}}(\sigma_2 \lambda_2^l) \cdot t] \exp[\bar{\mathbf{J}}(\sigma_1 \lambda_1^j) \cdot t] \} \delta \mathbf{x}(0).
 \end{aligned} \tag{18}$$

We define $S_{jl} = \mathbf{v}^{lT} \mathbf{u}^j$, so that $\mathbf{v}^l \mathbf{v}^{lT} \mathbf{u}^j \mathbf{u}^{jT} = \sum_j \mathbf{u}^j \mathbf{u}^{jT} S_{jl} S_{jl}$. Then Eq. (18) can be rewritten as

$$\delta \mathbf{x}(T) = \sum_{j,j'} \left\{ \mathbf{u}^{j'} \mathbf{u}^{j'T} \otimes \sum_l S_{j'l} S_{jl} \{ \exp[\bar{\mathbf{J}}(\sigma_2 \lambda_2^l) \cdot \tau_2] \exp[\bar{\mathbf{J}}(\sigma_1 \lambda_1^j) \cdot \tau_1] \} \right\} \delta \mathbf{x}(0). \tag{19}$$

Taking again $\delta \mathbf{x} = \mathbf{Q} \delta \mathbf{y}$, one eventually gets

$$\delta \mathbf{y}(T) = \sum_{j,j'} \left\{ \mathbf{e}^{j'} \mathbf{e}^{j'T} \otimes \sum_l S_{j'l} S_{jl} \{ \exp[\bar{\mathbf{J}}(\sigma_2 \lambda_2^l) \cdot \tau_2] \exp[\bar{\mathbf{J}}(\sigma_1 \lambda_1^j) \cdot \tau_1] \} \right\} \delta \mathbf{y}(0). \tag{20}$$

Remarkably, when $\mathbf{e}^{j'} \mathbf{e}^{j'T}$ acts on a vector, it actually picks its component on the direction \mathbf{e}^j and turns it into the direction $\mathbf{e}^{j'}$. Thus, one obtains

$$\delta \mathbf{y}^{j'}(T) = \sum_{j,l} S_{j'l} S_{jl} \{ \exp[\bar{\mathbf{J}}(\sigma_2 \lambda_2^l) \cdot \tau_2] \exp[\bar{\mathbf{J}}(\sigma_1 \lambda_1^j) \cdot \tau_1] \} \cdot \delta \mathbf{y}^j(0). \tag{21}$$

When τ_1 and τ_2 are large, we have

$$\begin{aligned}
 |\delta \mathbf{y}^{j'}(T)| &= \left| \sum_{j,l} \{ S_{j'l} S_{jl} \cdot \exp[\bar{\mathbf{J}}(\sigma_2 \lambda_2^l) \cdot \tau_2] \exp[\bar{\mathbf{J}}(\sigma_1 \lambda_1^j) \cdot \tau_1] \} \cdot \delta \mathbf{y}^j(0) \right| \\
 &\leq \sum_{j,l} \{ S_{j'l} S_{jl} \cdot \| \exp[\bar{\mathbf{J}}(\sigma_2 \lambda_2^l) \cdot \tau_2] \| \cdot \| \exp[\bar{\mathbf{J}}(\sigma_1 \lambda_1^j) \cdot \tau_1] \| \} \cdot |\delta \mathbf{y}^j(0)| \\
 &= \sum_{j,l} \{ S_{j'l} S_{jl} \cdot \exp[\Phi(\sigma_1 \lambda_1^j) \tau_1 + \Phi(\sigma_2 \lambda_2^l) \tau_2] \} \cdot |\delta \mathbf{y}^j(0)|.
 \end{aligned} \tag{22}$$

The stable synchronization demands the convergence of $|\delta \mathbf{y}^{j'}(T)|$ which accounts for the condition that: for each pair of $(j, l \geq 2)$, if $S_{jl} \neq 0$, then one should have

$$\tau_1 \Phi(\sigma_1 \lambda_1^j) + \tau_2 \Phi(\sigma_2 \lambda_2^l) < 0, \tag{23}$$

as stated in Eq. (4). In analogy, the condition could be directly extended to the general case of arbitrary number of configurations, as formulated by Eq. (5).

Condition of stable synchronization of fast switching networks. For the case of fast-switching, we also start from the situation that a network periodically switches between two configurations $\{\mathbf{G}_1, \tau_1, \sigma_1\}$ and $\{\mathbf{G}_2, \tau_2, \sigma_2\}$, while here τ_1 and τ_2 are sufficiently small. It has been found that the condition of stable synchronization for fast-switching networks is that the time average of the coupling matrices $\bar{\mathbf{G}} = \frac{1}{T}(\tau_1 \sigma_1 \mathbf{G}_1 + \tau_2 \sigma_2 \mathbf{G}_2)$ supports synchronization¹⁷.

Now, we look at a specific case that $\mathbf{G}_1 = \sum_j \lambda_1^j \mathbf{u}^j \mathbf{u}^{jT}$ and $\mathbf{G}_2 = \sum_j \lambda_2^j \mathbf{v}^j \mathbf{v}^{jT}$ share the same basis, i.e. $\mathbf{u}^j = \mathbf{v}^j$ for all j and therefore $S_{jl} = \delta_{jl}$. In this case, stable synchronization could be attained when for all the transverse modes one has

$$\Phi \left(\frac{\tau_1 \sigma_1 \lambda_1^j + \tau_2 \sigma_2 \lambda_2^j}{T} \right) < 0. \tag{24}$$

This result is readily extended to a general situation of networks fast switching among arbitrarily number of configurations. The condition of stable synchronization now is

$$\Phi \left(\frac{1}{T} \sum_{k=1}^L \tau_k \sigma_k \lambda_k^j \right) < 0, \tag{25}$$

where notations are similar to those in the Eq. (5) of the main text. We note that this case that the Laplacians of all the configurations share the same basis covers a large class of network whose coupling strength varies with time but structure fixes.

References

1. Boccaletti, S. *et al.* The Synchronization of Chaotic Systems. *Phys. Rep.* **366**, 1 (2002).
2. Mosekilde, E., Maistrenko, Y. & Postnov, D. Chaotic Synchronization: Application to Living Systems. *World Scientific Nonlinear Science Series A* (2002).
3. Pikovsky, A., Rosenblum, M. & Kurths, J. *Synchronization* (Cambridge University Press, Cambridge, England, 2003).
4. Dorogovtsev, S. N., Goltsev, A. V. & Mendes, J. E. F. Critical phenomena in complex networks. *Rev. Mod. Phys.* **80**, 1275 (2008).
5. Vicsek, A. *et al.* Novel Type of Phase Transition in a System of Self-Driven Particles. *Phys. Rev. Lett.* **75**, 1226 (1995).
6. Pikovsky, A. S., Rosenblum, M. G., Osipov, G. V. & Kurths, J. Phase synchronization of chaotic oscillators by external driving. *Physica (Amsterdam)* **104D**, 219 (1997).
7. Skardal, P. S., Taylor, D. & Sun, J. Optimal Synchronization of Complex Networks. *Phys. Rev. Lett.* **113**, 144101 (2014).
8. Zou, Y. *et al.* Basin of Attraction Determines Hysteresis in Explosive Synchronization. *Phys. Rev. Lett.* **112**, 114102 (2014).
9. Gu, C. *et al.* Heterogeneity induces rhythms of the weakly coupled circadian neurons. *Sci. Rep.* **6**, 21412 (2016).
10. Gu, C. *et al.* Noise Induces Oscillation and Synchronization of the Circadian Neurons. *PLoS ONE* **10**, e0145360 (2015).
11. Pecora, L. M. & Carroll, T. L. Master Stability Functions for Synchronized Coupled Systems. *Phys. Rev. Lett.* **80**, 2109 (1998).
12. Boccaletti, S. *et al.* Synchronization in dynamical networks: Evolution along commutative graphs. *Phys. Rev. E* **74**, 016102 (2006).
13. Porfiri, M. Stochastic synchronization in blinking networks of chaotic maps. *Phys. Rev. E* **85**, 056114 (2012).
14. Uriu, K., Ares, S., Oates, A. C. & Morelli, L. G. Dynamics of mobile coupled phase oscillators. *Phys. Rev. E* **87**, 032911 (2013).
15. Kohar, V. *et al.* Synchronization in time-varying networks. *Phys. Rev. E* **90**, 022812 (2014).
16. Zhang, X., Boccaletti, S., Guan, S. & Liu, Z. Explosive Synchronization in Adaptive and Multilayer Networks. *Phys. Rev. Lett.* **114**, 038701 (2015).
17. Stilwell, D. J., Bollt, E. M. & Roberson, D. G. Synchronization of Time-Varying Networks Under Fast Switching. *SIAM J. Appl. Dyn. Syst.* **5**, 140 (2006).
18. Frasca, M. *et al.* Synchronization of moving chaotic agents. *Phys. Rev. Lett.* **100**, 044102 (2008).
19. Fujiwara, N., Kurths, J. & Díaz-Guilera, A. Synchronization in networks of mobile oscillators. *Phys. Rev. E* **83**, 025101(R) (2011).
20. Markram, H., Wang, Y. & Tsodyks, M. Differential signaling via the same axon of neocortical pyramidal neurons. *Proc. Natl. Acad. Sci. USA* **95**, 5323 (1998).
21. Turrigiano, G. G. *et al.* Activity-dependent scaling of quantal amplitude in neocortical neurons. *Nature* **391**, 892 (1998).
22. Davis, G. W. Homeostatic control of neural activity: from phenomenology to molecular design. *Annu. Rev. Neurosci.* **29**, 307 (2006).
23. Tetzlaff, C., Kolodziejewski, C., Markelic, I. & Wörgötter, F. Time scales of memory, learning, and plasticity. *Biol. Cybern.* **106**, 715 (2012).
24. Mongillo, G., Barak, O. & Tsodyks, M. Synaptic theory of working memory. *Science* **319**, 1543 (2008).
25. Vazquez, F., Eguíluz, V. M. & Miguel, M. S. Generic absorbing transition in coevolution dynamics. *Phys. Rev. Lett.* **100**, 108702 (2008).
26. Masuda, N., Klemm, K. & Eguíluz, V. M. Temporal networks: slowing down diffusion by long lasting interactions. *Phys. Rev. Lett.* **111**, 188701 (2013).
27. Chen, L., Qiu, C. & Huang, H. B. Synchronization with on-off coupling: Role of time scales in network dynamics. *Phys. Rev. E* **79**, 045101(R) (2009).
28. Schröder, M. *et al.* Transient Uncoupling Induces Synchronization. *Phys. Rev. Lett.* **115**, 054101 (2015).
29. del Genio, C. I., Romance, M., Criado, R. & Boccaletti, S. Synchronization in dynamical networks with unconstrained structure switching. *Phys. Rev. E* **92**, 062819 (2015).
30. Nishikawa, T., Motter, A. E., Lai, Y.-C. & Hoppensteadt, F. C. Heterogeneity in oscillator networks: are smaller worlds easier to synchronize? *Phys. Rev. Lett.* **91**, 014101 (2003).
31. Nishikawa, T. & Motter, A. E. Network synchronization landscape reveals compensatory structures, quantization, and the positive effect of negative interactions. *Proc. Natl. Acad. Sci. USA* **107**, 10342 (2010).
32. Erdős, P. & Renyi, A. The Evolution of Random Graphs. *Publ. Math. Inst. Hung. Acad. Sci.* **5**, 17 (1960).
33. Barabási, A.-L., Albert, R. & Jeong, H. Mean-field theory for scale-free random networks. *Physica A* **272**, 173 (1999).

Acknowledgements

Work partially supported by the National Natural Scientific Foundation of China grants (Nos 11405059, 11135001, 11375066, 11305062, and 61503110).

Author Contributions

J.Z., Y.Z., S.G., Z.L. and S.B. conceived the methods and the research; J.Z. performed the numerical simulations; J.Z. and S.B. wrote the paper. All authors reviewed the Manuscript.

Additional Information

Supplementary information accompanies this paper at <http://www.nature.com/srep>

Competing financial interests: The authors declare no competing financial interests.

How to cite this article: Zhou, J. *et al.* Synchronization in slowly switching networks of coupled oscillators. *Sci. Rep.* **6**, 35979; doi: 10.1038/srep35979 (2016).



This work is licensed under a Creative Commons Attribution 4.0 International License. The images or other third party material in this article are included in the article's Creative Commons license, unless indicated otherwise in the credit line; if the material is not included under the Creative Commons license, users will need to obtain permission from the license holder to reproduce the material. To view a copy of this license, visit <http://creativecommons.org/licenses/by/4.0/>

© The Author(s) 2016